Spatiotemporal evolution and multiple self-focusing of ultrashort pulses in a resonant two-level medium

Yueping Niu,* Keyu Xia, Ni Cui, Shangqing Gong,† and Ruxin Li
State Key Laboratory of High Field Laser Physics, Shanghai Institute of Optics and Fine Mechanics, Chinese Academy of Sciences, Shanghai 201800, China
(Received 21 July 2008; published 30 December 2008)

The spatiotemporal evolutions of ultrashort pulses in two dimensions are investigated numerically by solving the coupled Maxwell-Bloch equations without invoking the slowly varying envelope approximation and rotating-wave approximation. For an on-axis $2n\pi$ sech pulse, local delay makes the temporal split 2π sech pulses crescent-shaped in the transverse distribution. Due to the transverse effect, the temporal split 2π sech pulses become unstable and experience reshaping during the propagation process. Then, interference occurs between the successive crescent-shaped pulses and multiple self-focusing can form.

DOI: 10.1103/PhysRevA.78.063835 PACS number(s): 42.65.Re, 42.65.Jx, 42.50.Md, 42.25.Bs

Since the pioneering work of McCall and Hahn [1,2], self-induced transparency (SIT) and area theorem for the evolution of light pulses have been the subjects of numerous studies [3–8]. Temporal reshaping effects, such as pulse breakup, pulse delays, and pulse compression, have been observed. In realistic experiments, however, transverse effects because of the beam radius and distribution of the field play important roles in the light-matter interaction process. Based on the coupled Maxwell-Bloch equations with the slowly varying envelope approximation (SVEA) and rotating-wave approximation (RWA), the influences of the transverse effects are investigated extensively [9–13]. Lamare *et al.* [12] revealed the dependence of the focusing distance and the maximal on-axis energy density on the interaction's parameters. In their work, the diaphragm effect at the edge of the pulse because of the transverse dependence of local SIT phenomena was proposed to interpret the focusing. On the other hand, there are so many studies that concentrate on the analytic solution of the Maxwell-Bloch equation which finally evolves into the nonlinear Schrödinger equation (NLSE) [14–19]. However, when the pulse envelope changes significantly over a time scale comparable to the period of the carrier, it is clear that the agreement between the NLSE based theory and the experimental results must break down. Up to now, a number of works have reported the limitations of the SVEA. Several different features arise in the full Maxwell solution that are absent in the standard SVEA models [4,6,20–23]. For example, Rothenberg *et al.* pointed out that the breakdown of the SVEA leads to a dramatic departure from the predicted symmetric development of the self-focusing pulse [20]. Forysiak and co-workers have reported the nonlinear focusing of femtosecond pulses as a result of self-reflection from a saturable absorber [24]. Recently, ultrafast transient population grating and ring-shaped population grating are demonstrated theoretically by us through the full-wave Maxwell-Bloch equations without any approximations [25,26].

In this paper, we will investigate the spatiotemporal evolution of ultrashort pulses with Gaussian transverse distribution in the two-dimensional geometry by solving the full-wave Maxwell-Bloch equations without the SVEA and RWA. Considering the interaction of a two-dimensional TE-polarized ultrashort pulse $\vec{E}(\vec{r},t)=E_x(y,z,t)$ with two-level atoms, we obtain the Maxwell equations for the electric and magnetic fields E_x, B_y, and B_z:

$$\partial_t B_y = -\partial_z E_x,$$

$$\partial_t B_z = \partial_y E_x,$$

$$\partial_t D_x = \frac{1}{\mu_0}(\partial_y B_z - \partial_z B_y), \tag{1}$$

where the z axis is the propagation direction and the y axis is the transverse direction. The nonlinear response of the two-

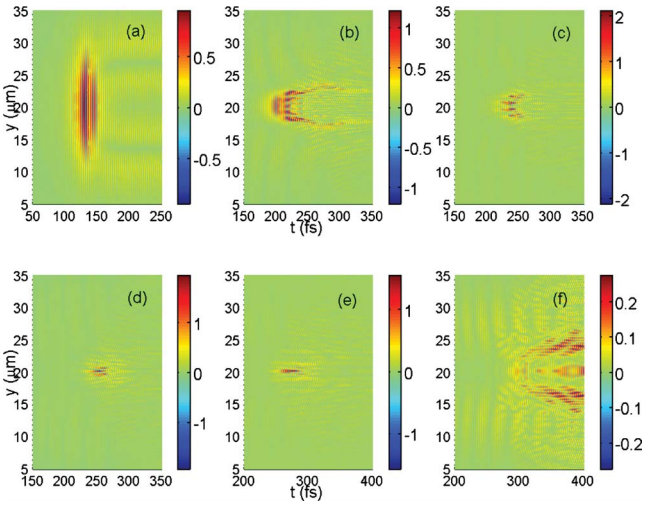

FIG. 1. (Color online) The two-dimensional profile of a 2π sech pulse at propagation distance of (a) $z=0$ μm, (b) 3 μm, (c) 4 μm, (d) 5 μm, (e) 6 μm, and (f) 10 μm. Other parameters are shown in the text.

*Corresponding author. niuyp@mail.siom.ac.cn
†Corresponding author. sqgong@mail.siom.ac.cn

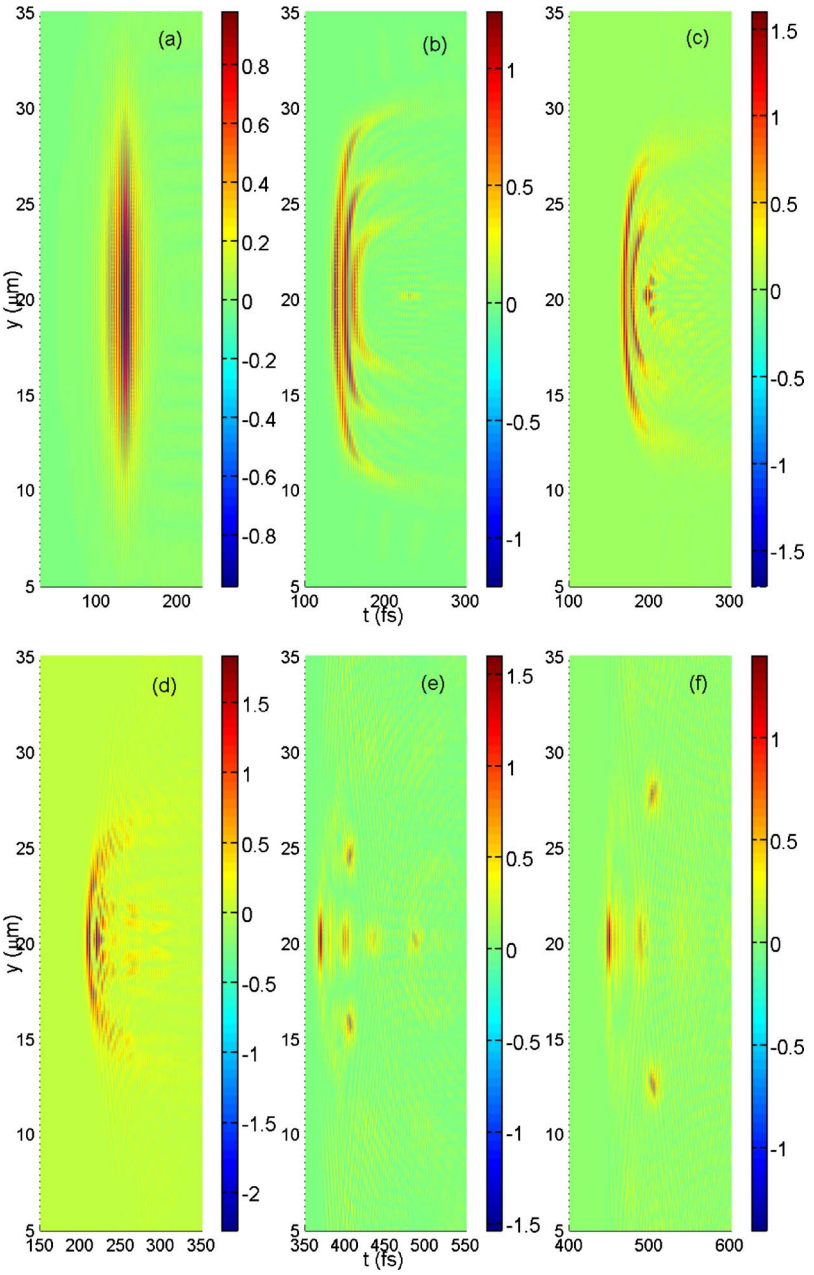

FIG. 2. (Color online) The two-dimensional profile of a 8π sech pulse at propagation distance of (a) $z=0$ μm, (b) 3.5 μm, (c) 10 μm, (d) 20 μm, (e) 60 μm, and (f) 80 μm. Other parameters are shown in the text.

level medium is included through the relation $D_x=\epsilon_0 E_x+P_x$, where the macroscopic polarization $P_x=-Ndu$ is determined by the Bloch equations beyond the standard approximations of SVEA and RWA:

$$\partial_t u = -\omega_{12} v - \gamma_1 u,$$

$$\partial_t v = \omega_{12} u - 2\frac{dE_x}{\hbar} w - \gamma_1 v,$$

$$\partial_t w = 2\frac{dE_x}{\hbar} v - \gamma_2 (w - w_0). \tag{2}$$

Here, ω_{12} is the atomic transition frequency, d is the dipole moment, and N is the density of the polarizable atoms. u and v are the dispersive and absorptive components of the off-diagonal density matrix element ρ_{12} while w represents the population difference between the two levels. w_0 represents the initial value of the population difference, and γ_1 and γ_2 means the polarization and population decay rate. For simplicity, we assume that the dipole moment d is aligned with the direction of the polarization of the applied electric field, i.e., the x axis and then the Rabi frequency is $\Omega=dE_x/\hbar$. We employ a standard finite-difference time-domain (FDTD) [27] approach to solve the full-wave Maxwell equations, and a fourth-order Runge-Kutta method to solve the Bloch equations [6]. Asymmetric boundary conditions [28] are imposed at the transverse boundaries, which are placed far enough away so that the optical intensity is negligible. The region of the medium is also assumed to be long enough such that the numerical reflection from the truncated end surface can be neglected. On the driving face ($z=0$) of the computational domain, the incident pulse has the form of [29]

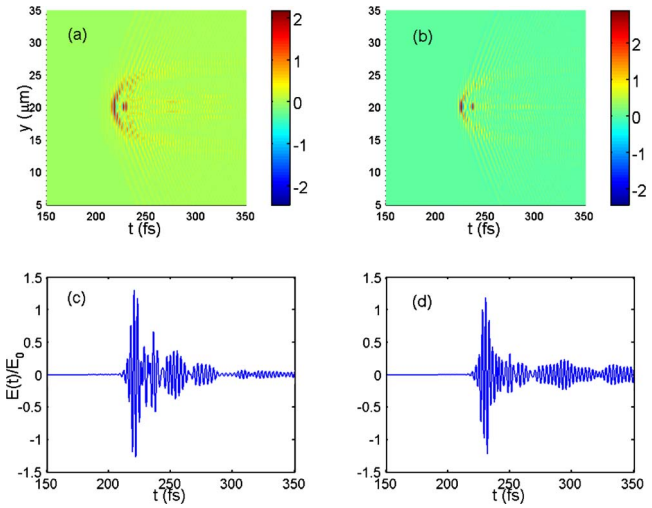

FIG. 3. (Color online) The two-dimensional profile of a 8π sech pulse at propagation distance of (a) $z=22$ μm, (b) $z=24$ μm. (c) and (d) are the corresponding one-dimensional pulse profiles at $y=18$ μm (22 μm).

$$E_x(y,z=0,t) = \sqrt{e}E_0 \exp\left(-\frac{(y-y_0)^2}{2r^2}\right)\mathrm{sech}\left(\frac{1.76(t-t_0)}{\tau_p}\right) \times \cos[\omega_p(t-t_0)], \quad (3)$$

where E_0 is the peak input electric field, r is the beam waist, and t_0 is the group delay. The choice of $t_0=120$ fs ensures that the field at $t=0$ is negligible. ω_p is the carrier frequency of the pulse and τ_p is the duration, i.e., the full width at half maximum (FWHM) of the intensity. The field transverse profile has its intensity peak at the axis $y=y_0$ and the on-axis pulse area is $A_p=dE_0\tau\pi/(1.76\hbar)$. We set $y_0=20$ μm to ensure that the field profile has zero intensity at $y=0$. In the following analysis, we adopt the field and material parameters based on Ref. [22]: $\tau_p=20$ fs, $\omega_p=2.3$ fs^{-1}, $d=2\times10^{-29}$ C m, $\gamma_1^{-1}=0.5$ ps, $\gamma_2^{-1}=1$ ps, and $N=8\times10^{19}$ cm^{-3}. The system is initialized with $u=0$, $v=0$, and $w_0=-1$. The cell size $\Delta z=0.03$ μm (about $\lambda/27$) and $\Delta y=0.1$ μm ($r/60$) is chosen to ensure accurate numerical results. The resulting time step Δt is set equal to 0.09 fs which meets the Courant condition. All the intensities considered here are in the order of 10^{12} W/cm^2. For such laser intensity, recent experiments on semiconductors have demonstrated that a description in terms of two-level systems has been able to reproduce the experimental results amazingly well [30,31]. Moreover, a few significant works that have studied this model can also be found in Refs. [4,6,22]. So, when the laser intensity is of the order of 10^{12} W/cm^2, the simple two-level system can provide an adequate description.

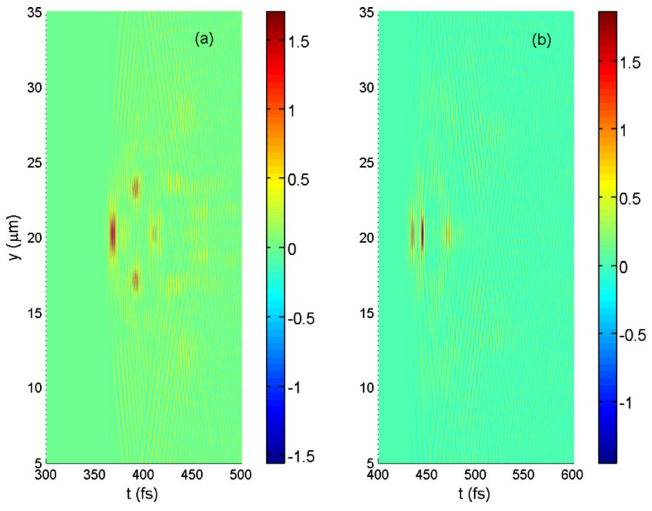

FIG. 4. (Color online) The two-dimensional profile of (a) 8π sech pulse with $r=7$ μm at $z=60$ μm and (b) 12π sech pulse with $r=6$ μm at $z=80$ μm.

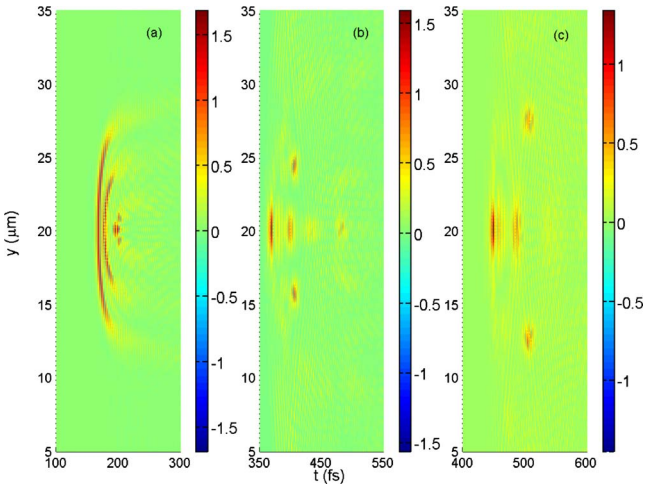

FIG. 5. (Color online) As in Fig. 2 but with a reduced grid-cell size and time step: $\Delta z=0.015$ μm, $\Delta y=0.05$ μm, and $\Delta t=0.04$ fs. (a) $z=10$ μm, (b) 60 μm, and (c) 80 μm.

A significant theory in the field of coherent resonant interaction is the SIT and the area theorem: when the envelope of the hyperbolic secant pulse has an area of $2n\pi$ ($n=1,2,3,\ldots$), then it propagates lossless; and the $2n\pi$ pulse will break up into separated 2π sech pulses. However, the temporal reshaping of experimental pulses is crucially affected by the transverse effect. As Fig. 1 shows, an initial 2π sech pulse with a beam waist of 6 μm evolves progressively into a crescent-shaped pulse since local delays are proportional to the inverse of the local Rabi frequency. At the same time, it begins to self-focus which results from the diffraction-induced inward flow of energy from the outer rings [12]. However, due to the transverse effect, the 2π sech pulse reshapes and breaks up temporally during the propagation process. Hence although the whole pulse experiences self-focusing initially, the temporal profile of the 2π sech pulse is deformed because of the transverse energy distribution and then defocusing occurs and all the energy dissipates in the space finally.

In the following, let us consider a $2n\pi$ sech pulse, e.g., $n=4$, with a beam waist of $r=6$ μm. The spatiotemporal evolution is more complicated, which can be seen from Fig. 2. Because the pulse has an area of 8π, it breaks up into four successive 2π pulses with decreasing intensities and beam

waists. The four individual pulses have their own transverse characteristic beam waist and each pulse may undergo self-focusing at its own distance in the y axis if its characteristic beam waist is large enough. This can be seen clearly from Figs. 2(b)–2(d). However, because the transverse effect causes the individual pulses to reshape and break up temporally, their energy then decreases during the propagation process. For those that the energy is below the self-focusing threshold, defocusing occurs and hence the corresponding focus in the y axis disappears. This process can also be discerned from Figs. 2(b)–2(d).

With further propagation, such as at the distance of $z=60$ μm, a different phenomenon is presented. Except for the focus mentioned above, extra foci come into being which locate in the y axis and also its two sides symmetrically [Figs. 2(e) and 2(f)]. In order to explore the physical reason, we conduct detailed analysis and demonstrate in Fig. 3 the related pulse profile. Attention should be paid to the following three points. On the one hand, because the four successive 2π pulses have decreasing intensities, the former pulses propagate faster than the latter ones. On the other hand, due to the local delay caused by the monotonically decreasing transverse energy distribution, each of the pulses becomes crescent-shaped and the outer part that is far from the y axis propagates slower than the inner part which is near the axis. Finally, because of the transverse effect, nearly all the individual crescent-shaped 2π pulses break up temporally and a different degree of reshaping can be found. Then, the reshaped pulses overlap at $y=0$ and $y=18$ μm (22 μm). As we know, the 2π pulses split from the $2n\pi$ pulse have the same frequency, hence the overlapped pulses can interfere and build up in intensity. Figures 3(c) and 3(d) are the corresponding one-dimensional pulse profile at $y=18$ μm (22 μm). From the two figures, one can see that the first and second pulses overlap more seriously with further propagation and hence the intensity at $z=24$ μm is higher than that of $z=22$ μm. When the intensity of the interfered pulses is higher than that of the self-focusing threshold, extra foci come into being.

We also simulate the propagation of pulses with other beam waist and pulse areas. Similar results are found except that the number of foci and their locations can be influenced greatly by those parameters. Figure 4(a) is the pulse profile resulting from a 8π sech pulse with $r=7$ μm while Fig. 4(b) is the pulse profile from a 12π sech pulse with $r=6$ μm. Clearly no extra focus is presented in both sides of the y axis when a 12π pulse is considered while multiple interferences occur which leads to multiple self-focusing when the beam waist is changed. Certainly, other pulse areas and beam waist can lead to different numbers of foci which locate at different positions.

In order to check the spatial and temporal convergence of our numerical simulation, we simulate the propagation process of the above $8\pi/6$ μm sech pulse with a 50% reduced grid-cell size (i.e., $\Delta z=0.015$ μm, $\Delta y=0.05$ μm, and $\Delta t=0.04$ fs) in Fig. 5. Compared with those of Fig. 2, almost no alterations of the propagation characteristics can be found, which demonstrate the accuracy of our numerical results.

In conclusion, we have investigated the spatiotemporal evolution of ultrashort pulses numerically without invoking any approximations. Multiple self-focusing in the transverse axis and also its two sides are found to be present. Our analysis shows that it is the transverse effect that leads to the break up of a 2π sech pulse temporally and then interference occurs between the successive crescent-shaped pulses. With further propagation, the interfered pulse builds up and then self-focuses in the transverse axis and also its two sides occurs.

ACKNOWLEDGMENTS

This work was supported by the National Natural Science Foundation of China (Grant No. 60708008 and No. 10874194), the Project of Academic Leaders in Shanghai (Grant No. 07XD14030), 973 Program (Grant No. 2006CB806000 and No. 2006CB921104), and the Knowledge Innovation Program of the Chinese Academy of Sciences.

[1] S. L. McCall and E. L. Hahn, Phys. Rev. Lett. **18**, 908 (1967).
[2] S. L. McCall and E. L. Hahn, Phys. Rev. **183**, 457 (1969).
[3] G. L. Lamb, Jr., Rev. Mod. Phys. **43**, 99 (1971).
[4] R. W. Ziolkowski, J. M. Arnold, and D. M. Gogny, Phys. Rev. A **52**, 3082 (1995).
[5] R. G. Flesch, A. Pushkarev, and J. V. Moloney, Phys. Rev. Lett. **76**, 2488 (1996).
[6] S. Hughes, Phys. Rev. Lett. **81**, 3363 (1998).
[7] J. Xiao, Z. Wang, and Z. Xu, Phys. Rev. A **65**, 031402(R) (2002).
[8] S. A. Skobelev, D. V. Kartashov, and A. V. Kim, Phys. Rev. Lett. **99**, 203902 (2007).
[9] S. L. McCall and E. L. Hahn, Phys. Rev. A **2**, 861 (1970).
[10] N. Wright and M. C. Newstein, Opt. Commun. **9**, 8 (1973).
[11] H. M. Gibbs, B. Bölger, F. P. Mattar, M. C. Newstein, G. Forster, and P. E. Toschek, Phys. Rev. Lett. **37**, 1743 (1976).
[12] J. de Lamare, M. Comte, and P. Kupecek, Phys. Rev. A **50**, 3366 (1994).
[13] J. de Lamare, P. Kupecek, and M. Comte, Phys. Rev. A **51**, 4289 (1995).
[14] P. L. Kelley, Phys. Rev. Lett. **15**, 1005 (1965).
[15] Y. Silberberg, Opt. Lett. **15**, 1282 (1990).
[16] J. K. Ranka, R. W. Schirmer, and A. L. Gaeta, Phys. Rev. Lett. **77**, 3783 (1996).
[17] A. A. Zozulya, S. A. Diddams, A. G. Van Engen, and T. S. Clement, Phys. Rev. Lett. **82**, 1430 (1999).
[18] A. A. Ishaaya, T. D. Grow, S. Ghosh, L. T. Vuong, and A. L. Gaeta, Phys. Rev. A **75**, 023813 (2007).
[19] A. A. Ishaaya, L. T. Vuong, T. D. Grow, and A. L. Gaeta, Opt. Lett. **33**, 13 (2008).
[20] J. E. Rothenberg, Opt. Lett. **17**, 1340 (1992).
[21] J. K. Ranka and A. L. Gaeta, Opt. Lett. **23**, 534 (1998).

[22] V. P. Kalosha and J. Herrmann, Phys. Rev. Lett. **83**, 544 (1999).
[23] G. Slavcheva, J. M. Arnold, I. Wallace, and R. W. Ziolkowski, Phys. Rev. A **66**, 063418 (2002).
[24] W. Forysiak, J. V. Moloney, and E. M. Wright, Opt. Lett. **22**, 239 (1997).
[25] K. Xia, Y. Niu, R. Li, S. Jin, and S. Gong, Phys. Rev. A **75**, 053816 (2007).
[26] K. Xia, Y. Niu, N. Cui, and S. Gong, Phys. Rev. A **77**, 013802 (2008).
[27] A. Taflove, *Computational Electrodynamics: The Finite-Difference Time-Domain Method*, Third Edition (Artech House, Boston, 1995).
[28] W. W. Lui, K. Yokoyama, and W. P. Huang, IEEE J. Sel. Top. Quantum Electron. **2**, 174 (1996).
[29] G. P. Agrawal, Phys. Rev. Lett. **64**, 2487 (1990).
[30] O. D. Mücke, T. Tritschler, M. Wegener, U. Morgner, and F. X. Kärtner, Phys. Rev. Lett. **89**, 127401 (2002).
[31] T. Tritschler, O. D. Mücke, and M. Wegener, Phys. Rev. A **68**, 033404 (2003).